Talanta 121 (2014) 50–55

Contents lists available at ScienceDirect

Talanta

journal homepage: www.elsevier.com/locate/talanta

Polyamidoamine dendrimers as sweeping agent and stationary phase for rapid and sensitive open-tubular capillary electrophoretic determination of heavy metal ions

Ying Ge, Yujun Guo, Weidong Qin*

College of Chemistry, Beijing Normal University, No. 19, Xinjiekou Wai Street, Beijing 100875, PR China

ARTICLE INFO

Article history:
Received 16 September 2013
Received in revised form
19 December 2013
Accepted 20 December 2013
Available online 30 December 2013

Keywords:
Polyamidoamine dendrimer
Dual sweeping
Open-tubular capillary electrochromatography
Heavy metal

ABSTRACT

Polyamidoamine (PAMAM) dendrimer generation 2.5 was synthesized and evaluated as sweeping agent for in-column enrichment and as stationary phase for capillary electrochromatographic separation of heavy metal ions, viz., Pb(II), Cu(II), Hg(II), Zn(II) and Co(II), in a running buffer containing 4-(2-pyridylazo)resorcinol (PAR) as a chromogenic reagent. During experiment, a plug of aqueous PAMAM generation 2.5 solution was first introduced to the capillary, followed by electrokinetic injection of the heavy metal ions under a positive voltage. In this step, PAMAM acted as a sweeping agent, stacking the metal ions on the analyte/PAMAM boundary by forming metal ion–PAMAM complexes. The second preconcentration process occurred when PAR, a stronger ligand, moving toward the injection end under the electric field, reached and re-swept the metal ion–PAMAM zone, forming metal ion–PAR complexes. During separation, the neutral PAMAM moved toward the detector with the electroosmotic flow, dynamically coating the capillary wall, forming stationary phases that affected the separation of the metal ions. Due to the function of PAMAM, the detection sensitivity and resolution of the heavy metal ions improved significantly. Under the optimum conditions, the detection limits were 0.299, 0.184, 0.774, 0.182 and 0.047 μg/L for Pb(II), Cu(II), Hg(II), Zn(II) and Co(II), respectively. The method was successfully applied to the determination of heavy metals in snow, tap and rain water samples.

1. Introduction

Some heavy metals in minute amounts are essential micronutrients needed by humans and animals for biological activities, but are poisonous at higher concentrations, for example, copper, cobalt and zinc. Most other heavy metals, e.g., mercury and lead, are determined to be toxic, dangerous to human health and environment. To assess the degree of contamination, substantial efforts have been directed to the analytical techniques capable of determining heavy metals at trace levels in various sample matrices, including tap water and environmental components such as snow, rain and surface waters [1,2].

Capillary electrophoresis (CE) is an increasingly used separation technique that possesses the advantages of superior separation efficiency within shorter time, simplicity in instrumentation and lower consumption of reagents. CE analysis of heavy metal ions, however, is not a trivial task. Metal ions of same charge, in particular those transition metal ions, have only slight differences in electrophoretic mobilities. To improve resolution, various complexing agents have to be introduced into the running buffer. Examples are ethylenediaminetetraacetic acid, 18-crown-6 ether, hydroxycarboxylic acids, amino acids, and oxalic acid [2]. Another issue should be concerned with CE analysis is its inherently poor detection sensitivity owing to the small sample volume and the short optical path of the capillary (for optical detection), practically hindering the direct analysis of heavy metal ions usually at μg/L or even ng/L levels in real samples. A number of ideas for preconcentration, based on either off-column [3] or in-column [4] modes, have been proposed to address this problem. In-column sample preconcentration represents an effective and versatile approach which is typically categorized into field amplified sample stacking (FASS) [1], transient isotachophoresis (t-ITP) [5], dynamic pH junction and sweeping [6]. Sweeping was introduced by Quirino and Terabe [7]; it is now an important in-column enrichment strategy based on the electrophoresis-induced interaction between analytes and sweeping agents [8]. Note that all these techniques have variations. The so-called field amplified sample injection (FASI), for example, is the head-column FASS, during which the analytes in a matrix of lower conductivity than the separation buffer are electrokinetically introduced into capillary. In addition, the techniques can be combined for higher enrichment factors.

Polyamidoamines (PAMAMs) are dendritic molecules possessing precise structures and high geometric symmetry [9]. Their properties in CE running buffer were studied [10,11] and they have

Abbreviations: PAMAM, polyamidoamine dendrimer; PAR, 4-(2-pyridylazo)resorcinol; OTCEC, open-tubular capillary electrochromatography

* Corresponding author. Tel.: +86 10 58802531; fax: +86 10 58802075.
E-mail address: qinwd@bnu.edu.cn (W. Qin).

0039-9140/$ - see front matter © 2013 Elsevier B.V. All rights reserved.
http://dx.doi.org/10.1016/j.talanta.2013.12.041

been employed as pseudostationary phases to separate aromatic hydrocarbons [12], positional isomers of neutral phenols [13], parabens [14], amino acids [15] and proteins [16,17], providing better separation efficiencies than the conventional ones. Recently, they were also used as sweeping agents for in-line enrichment of DNA fragments [18]. Besides interacting with organic compounds, PAMAMs can chelate with metal ions [19,20]. The work of Shcharbin et al. [21] further indicated that the chelates decomposed in the presence of a large amount of sodium ion through ion exchange. It can be inferred from these findings that when employed in CE PAMAMs can influence the migration and perhaps even detection of metal ions.

We studied in this report the influence of PAMAMs on the separation and detection of the heavy metal ions, by introducing a short plug of PAMAM into the capillary prior to sample injection as sweeping agents and as stationary phases in open-tubular capillary electrochromatography. The influences of separation conditions were investigated and optimized. Finally, the method was demonstrated for the determination of heavy metals in snow, tap and rain water samples.

2. Experimental

2.1. Reagents and chemicals

All chemicals were of analytical grade and were used as received. 4-(2-pyridylazo)resorcinol (PAR, >99%) was purchased from Alfa Aesar (Beijing, China). Sodium tetraborate ($Na_2B_4O_7$), boric acid (H_3BO_3), sodium hydroxide (NaOH), phenol, ethanol, methanol and the salts of heavy metals, mercuric(II) nitrate, lead (II) nitrate, cobalt(II) chloride, copper(II) sulfate and zinc(II) acetate (all >99%), were products of Beijing Chemical Plant (Beijing, China). L-Tryptophan (Trp, >99%) and L-Cysteine (Cys, ≥99%) were supplied by Biodee (Beijing, China). L-Histidine (His, >99%) was obtained from Beijing Dingguochangsheng Biotechnology (Beijing, China). Ethylenediamine and methyl acrylate were bought from Tianjin Fuchen Chemicals (Tianjin, China). The stock solutions of heavy metal standards were prepared in triple distilled water at 100 mg/L, and PAR at 10 mM was prepared in ethanol. All working solutions were filtered through 0.45 μm filters (Jiu Ding High Tech., Beijing, China) before use.

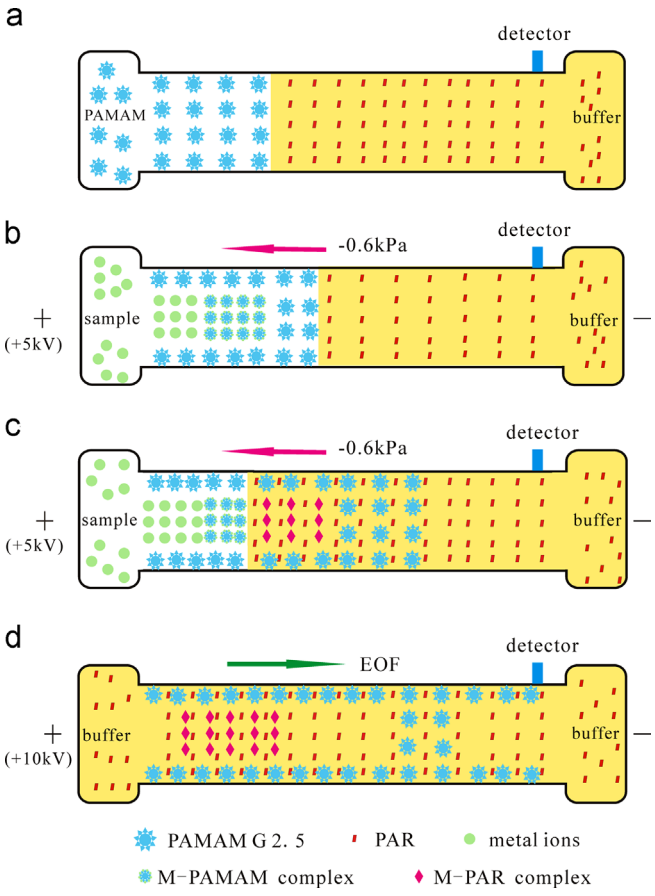

Fig. 1. Evolution of PAMAM- and PAR-induced dual sweeping with electrokinetic injection and OTCEC (not to scale). See Section 2.6 for details.

2.2. Synthesis of PAMAMs

PAMAMs of generations 0.5, 1.5, 2.5 and 3.5 employed in the experiment were synthesized and purified according to the procedures described in the report elsewhere [22] with slight modifications. It started from a two-step process: (I) exhaustive Michael addition to an ethylenediamine initiator core with excessive methyl acrylate, forming a tetraester, and (II) amidation of the product with large excesses of ethylenediamine, yielding amine-terminated generation zero dendrimer (PAMAM G 0). Based on this mechanism, PAMAM G 0.5 could be obtained from a Michael addition on G 0, and the progressive amidation/Michael addition cycles from G 0.5 generated higher generations of ester-terminated dendrimers (PAMAM G *n*.5, where *n* is an integer). In order to remove the excessive reactants, the product of each step was dissolved in methanol and purified with a rotary vacuum evaporator. Structures of the products (please refer to Supplementary information for ^{1}HNMR data) were identified using a Bruker Advance III-400 MHz NMR spectrometer (Rheinstetten, Germany).

2.3. Water samples

Tap water was collected directly from the laboratory. The snow sample was collected 2 h after snowing on December 29, 2012, on the campus of Beijing Normal University. The sampling site was about 100 m from a road of moderate traffic volume. The snowflakes were placed in a clean screw-capped centrifuge tube (13 cm × 3.5 cm i.d.) and stored at −15 °C. Before use, an aliquot of snow sample was precisely weighed and thawed at room temperature. Rain water was collected about 60 min from the onset of the raining at the top of the laboratory building on the campus on June 24, 2013; it was stored in a clean screw-capped

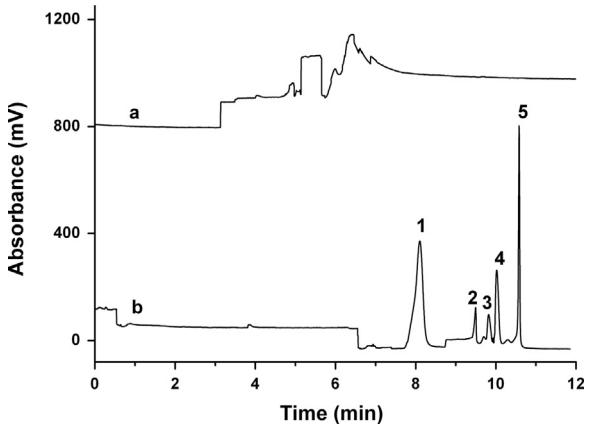

Fig. 2. Influence of PAMAM. Running buffer: 21 mM Trp, 7 mM NaOH and 0.22 mM PAR at pH 9.25. Triple distilled water (a) or PAMAM (b) plug was hydrostatically introduced at 22 cm × 20 s; FASI of metal ions was performed at +5 kV × 180 s, with a hydrodynamic backpressure at −0.6 kPa. Peak identities: 1, Pb(II); 2, Cu(II); 3, Hg(II); 4, Zn(II); 5, Co(II). Traces are offset for clarity.

centrifuge tube under refrigeration before use. All samples were filtered with a 0.45 μm filter before analysis.

Recoveries (*R*%) of heavy metal ions from the water samples were estimated on the basis of three spiking levels, using

$$R\% = \frac{S_2 - S_1}{S_0} \times 100 \quad (1)$$

where S_1 and S_2 are the peak areas of a metal ion in unspiked and spiked samples, respectively; S_0 is the peak area of this metal ion prepared in triple distilled water at the spiking concentration.

2.4. Capillary electrophoresis

CE analyses were performed on a DW-P303-1ACD8 high voltage supply (Dongwen High Tech., Tianjin, China), equipped with a homemade photometric detector which was described elsewhere [23]. Briefly, the light with maximum emission wavelength at 527 nm from the light-emitting diode (LED, Shifeng Corp., Shenzhen, China) was focused by two plano-convex lenses (25.4 mm diameter × 30 mm effective focal length, Golden Way Scientific, Beijing, China) on the detection window of the capillary, which was aligned on the detector block. The transmitted light was detected by a photodiode (Qingyue, Shanghai, China), signal from which was picked up by an operational amplifier (AD708, Analog Devices, MA, USA) and fed to a logarithmic amplifier (LOG102, Texas Instruments, TX, USA). The output signal from the detector was collected by an IBM PC compatible computer via a CT22 data acquisition unit (Qianpu, Jiangsu, China), and was processed with HW2000 chromatography station (Qianpu). The preconcentration and separation were performed in a 45.0 cm (effective length 38.0 cm) fused-silica capillary (75 μm i.d., Yongnian Photoconduction Fibre, Hebei, China). The fresh capillary was conditioned sequentially with 0.5 M NaOH and triple distilled water for 20 min. It was rinsed with running buffer for 15 min before experiments every day. Between consecutive runs, it was flushed with running buffer for 2 min for reproducible results.

The length of the PAMAM plug introduced was estimated based on the injection height and the duration, with the free software (CE Expert) provided by Beckman [24]. The migration velocity v was obtained by

$$v = \mu U / L \quad (2)$$

where, μ, U and L are the mobility, the voltage applied across the capillary and the capillary length, respectively.

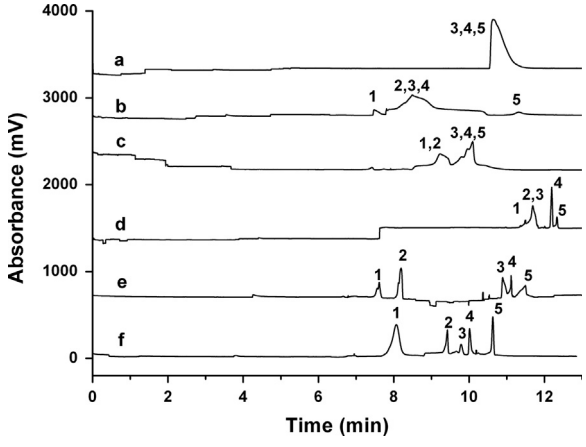

Fig. 3. Influence of background electrolyte. (a) 15 mM His–NaOH (pH 6.37); (b) 25 mM Trp–borate (titrated with NaOH to pH 9.23); (c) 12 mM $Na_2B_4O_7$–H_3BO_3 (pH 9.20); (d) 32 mM Trp–Cys–NaOH (pH 9.05); (e) 15 mM phenol–NaOH (pH 9.77); and (f) 28 mM Trp–NaOH (pH 9.25). Other conditions were the same as trace b of Fig. 2.

2.5. Inductively coupled plasma-mass spectrometry (ICP-MS)

An Agilent 7500ce quadrupole mass spectrometer (Agilent Technologies, CA, USA) was employed for verification and comparison. The operation parameters: RF power, 1350 W; plasma gas flow, 15 L/min; auxiliary gas flow, 0.9 L/min; carrier gas flow, 1.2 L/min; sampling depth 7.0 mm; octopole bias, −17 V; and quadrupole bias −15 V.

2.6. Dual sweeping-open-tubular capillary electrochromatography (OTCEC)

In Step a, the capillary was first filled with running buffer containing PAR. Then, a plug of PAMAM solution was loaded by 22 cm × 20 s, corresponding to 21.52 mm in length (Fig. 1a). Step b, the anodic reservoir was filled with sample solution and a positive voltage (+5 kV) was applied across the capillary to electrokinetically inject the metal ions (under FASI mode). Meanwhile, a backpressure (−0.6 kPa) was applied at the injection end, generating a flow at −0.29 mm/s in order to avoid the solutes migrating far away from the injection end by the cathodic electroosmotic flow (EOF, 0.47 mm/s) while preventing PAR (moving at −0.25 mm/s) and the metal ion–PAR (M–PAR) complexes from moving out of the capillary. At the beginning of the FASI, the introduced metal ions were stacked by forming metal ion–PAMAM (M–PAMAM) complexes at the sample/PAMAM boundary. This procedure can be termed sweeping – by the partial-filling PAMAM. It worked until after 85 ± 3.4 s, when negatively charged PAR electrophoretically moving toward the injection end ultimately reached the right edge of M–PAMAM zone. At this moment, another enrichment procedure took place (Step c). Because the binding constants of M–PAR are normally several orders higher than those of M–PAMAM [21], the PAMAM-bound metal ions were released and simultaneously bound by PAR and stacked at the metal ion/PAR boundary, where the subsequently injected heavy metal ions were directly swept by PAR through forming M–PAR complexes. Step d, after injection, the anodic reservoir was filled with running buffer, and a separation voltage (+10 kV) was applied across the capillary. The neutral PAMAM G 2.5 migrated toward the detector, driven by EOF, followed by negative M–PAR complexes. The O–Si–O bond on the inner silica surface is somewhat hydrophobic [25], leading to wall-adsorption of the highly hydrophobic PAMAM molecules. The immobilized dendrimers could act as stationary phase, interact with the M–PAR complexes and influence the separation. Therefore, the CE separation was under OTCEC mode.

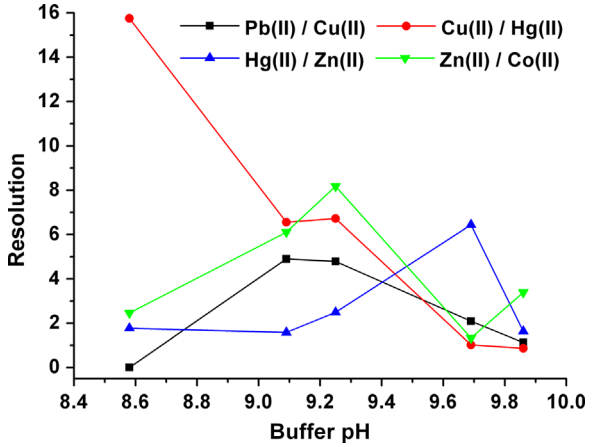

Fig. 4. Influence of buffer pH. The buffer concentrations under different pH were kept at 28 mM. Other conditions were the same as trace b of Fig. 2.

Table 1
The analytical figures of merit of the method.

	Pb(II)	Cu(II)	Hg(II)	Zn(II)	Co(II)
LOD (μg/L (nM))	0.299 (1.44)	0.184 (2.90)	0.774 (3.85)	0.182 (2.78)	0.047 (0.799)
MCL_1 (μg/L) [35]	10	1000	1	1000	/
MCL_2 (μg/L) [36]	15	1300	2	5000	/
Reported LODs with enrichment protocols (μg/L)	44 [6]	78 [6]	2.32 [1], 1.7 [33]	0.8 [34], 119 [6]	38 [6]
Linear range (mg/L)	2.5×10^{-3}–2.5	1×10^{-3}–0.5	5×10^{-3}–2.5	5×10^{-4}–0.5	2.5×10^{-4}–0.1
Intercept ($\times10^5$)	1.49 ± 0.93	0.68 ± 0.1	0.6 ± 0.05	0.46 ± 0.1	10.2 ± 0.2
Slope ($\times10^6$)	3.69 ± 0.09	2.9 ± 0.05	0.49 ± 0.0048	23.3 ± 0.6	22.6 ± 0.3
r^2	0.9953	0.9982	0.9994	0.9947	0.9987
Intra-day precision (RSD%, n=5)					
Migration time	1.66	1.21	1.15	2.06	1.64
Peak area	5.88	10.80	11.79	10.70	11.48
Inter-day precision(RSD%, 3 days, $n=3\times5=15$)					
Migration time	2.81	1.01	2.03	1.96	2.26
Peak area	11.99	10.82	11.50	12.87	10.56

Table 2
Analysis of real samples.

	Pb(II)	Cu(II)	Hg(II)	Zn(II)	Co(II)
Concentration found (μg/L) by CE/ by ICP-MS					
Rain water	ND/ND[a]	34.12/34.92	ND/ND	446.1/473.2	ND/ND
Snow water	ND/ND	23.37/22.58	ND/ND	53.66/54.71	ND/ND
Tap water	ND/ND	38.92/38.90	ND/ND	272.7/281.7	ND/ND
Recovery (%)					
Spiked (mg/L)	0.05/0.5/1	0.01/0.05/0.1	0.05/0.1/0.5	0.01/0.05/0.1	0.005/0.01/0.05
Snow water	103.1/101.1/103.7	108.5/100.9/99.2	86.7/88/100.3	96.4/96.2/105.5	97.7/101.3/97.9
Rain water	92.4/103.9/99.2	98.3/96.1/99.6	98.1/100.8/91.1	103.7/102.5/100.8	99.8/100.6/106.7
Tap water	102.2/99.3/102.3	99.1/93.6/98.6	93.2/101.5/101.4	96.5/92.5/103.9	104.7/101.9/99.9

[a] Not detected.

3. Results and discussion

3.1. Influence of PAMAM

Fig. 2 indicated that when a water plug was introduced prior to the electrokinetic sample injection, low, broad, tailing, overlapping peaks were obtained, accompanied by the elevated baseline after the last peak (trace a, from 8 min). The M–PAR complexes were negatively charged in the running buffer, and the electrostatic repulsion prevented their adsorption to the negative silica wall. Nonetheless, there were in the sample zone, co-existing with M–PAR, free heavy metal ions, whose concentrations were determined by the respective binding constants. The free heavy metal ions are highly susceptible to wall-adsorption [26]. It was reported by Iki et al. [27] that for some weak M–PAR complexes, the wall-adsorption of the free metal ions was so strong that no peaks could be detected in buffers devoid of PAR. Our results implied that Zn (II) interacted with silica wall at low adsorption/desorption kinetics (tailing peak in trace a), and Co(II) might irreversibly adsorb to the capillary surface, as evidenced by the raised baseline.

When the pre-introduced water was replaced with the PAMAM solution, sharp, well-defined peaks were observed (trace b). It was also found that under this operation mode the EOF mobility of the bulk running buffer decreased, from 0.000567 $cm^2V^{-1}s^{-1}$ to 0.000427 $cm^2V^{-1}s^{-1}$, implying wall-adsorption of the neutral PAMAM G 2.5. The dynamic PAMAM coating largely favored higher separation efficiency of the metal ions, because at the PAMAM surface fast ion exchange might take place between the background sodium and the free heavy metal ions [21]. Another interesting phenomenon is that the peak of last solute Co(II) is obviously slimmer, which can be attributed to different M–PAR binding constants. The binding constants of PAR to Pb(II), Cu(II) and Zn(II) are lower [26,28], and broad peaks might be generated corresponding to weak chelates [26].

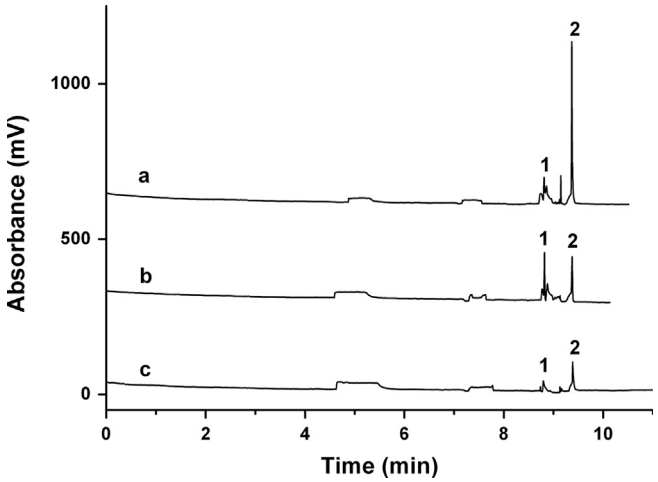

Fig. 5. Representative electropherograms of rain (a), tap (b) and snow water (c). Peak identities: 1, Cu(II); 2, Zn(II). Other conditions were the same as trace b of Fig. 2.

During separation, PAMAM G 2.5 as stationary phase influenced migration velocities of the analytes and, thereby, affected the selectivity of the method (Figs. S1–S3 of the Supplementary information). In addition, the separation performances were dependent on the PAMAM generations (Fig. S1), because the numbers of surface functional groups and intramolecular cavities vary with PAMAM generation. Experimental results suggested that introducing a 2.15-cm plug of 5 mM PAMAM G 2.5 could provide the best effects for both preconcentration and separation.

3.2. Selection of background electrolyte

To obtain best separation performance, six background electrolyte systems were investigated, i.e., His–NaOH, Trp–borate, $Na_2B_4O_7$–H_3BO_3, Trp–Cys–NaOH, phenol–NaOH and Trp–NaOH. The analytes had close mobilities in His–NaOH, Trp–borate and $Na_2B_4O_7$–H_3BO_3 buffers; therefore, no acceptable separation could be achieved (Fig. 3). Regarding Trp–Cys–NaOH, four of the five metal ions could be detected, but with narrow separation window. The five heavy metal ions were baseline resolved with phenol–NaOH; however, the peak of Co(II) broadened and the overall separation efficiency (theoretical plate number) was low. Fig. 3 indicates that Trp–NaOH buffer offered satisfactory resolution with better efficiency. Both Trp and Cys could form complex with metal ions [29,30], our experiments suggested that the Trp–metal interaction improved the separation of the metal ions studied, and therefore Trp–NaOH was selected for the further method development.

3.3. Influence of PAR

PAR is a commonly employed chromogenic reagent, which can act as a terdentate or bidentate ligand, forming stable chelates with a wide variety of metal ions through its three protonation sites, one pyridinic nitrogen and two phenolic oxygens [31,32]. Increasing the PAR concentration from 0.1 mM to 0.22 mM, the separation time reduced while separation efficiency and resolution improved (Fig. S4). The five heavy metal ions were baseline separated in the presence of 0.22 mM PAR. Further addition of PAR to buffer resulted in merging peaks of Hg(II) and Zn(II) and sharply decreased Cu(II) signal.

3.4. Effect of buffer pH and concentration

The effect of pH was investigated in the range between 8.58 and 9.86, by changing the molar ratio of the buffering components Trp and NaOH. Increasing buffer pH led to fast analysis (owing to the accelerated EOF), improved resolution between the first two peaks, Pb(II) and Cu(II), and high separation efficiency of all the metal ions until pH 9.25 (Fig. 4), under which all the peaks were baseline resolved at the highest overall peak intensity. Higher buffer pHs resulted in broaden peaks and deteriorated detectability; moreover, the peaks of Cu(II) and Hg(II) partly merged. Basic environment is needed for M–PAR complexation; in strong alkaline buffer, however, hydrolysis of the heavy metal ions might become significant, which would negatively affect the M–PAR chelation, causing low detection sensitivity and separation efficiency. We studied the influence of buffer concentration at a fixed pH value of 9.25, and found that the buffer concentration at 28 mM was optimal (Section 5 of the Supplementary information).

3.5. Performance and application

We investigated the analytical performances of the developed method under the optimized buffer conditions, i.e., 21 mM Trp, 7 mM NaOH and 0.22 mM PAR at pH 9.25. The limit of detection (LOD) was defined as the analyte concentration that produces a peak having a height equal to three times the standard deviation of the baseline noise. As listed in Table 1, the LODs of the five metal ions were 0.047, 0.182, 0.184, 0.299, and 0.774 μg/L for Co(II), Zn(II), Cu(II), Pb(II) and Hg(II), respectively, which were lower than the previous works [1,6,33,34]. The relatively high detection sensitivity of cobalt originated from the stable Co–PAR chelation; whereas the high LOD of Hg(II) might be the consequence of the low Hg–PAR chelating constant. Nonetheless, due to the dual sweeping strategy favoring the enrichment and to the dynamic PAMAM coating effectively suppressing the wall-adsorption, the detection sensitivity of Hg(II) was still high – it is to the best of our knowledge the most sensitive PAR-based photometric detection for CE analysis of mercury, even superior to amperometric detection [33]. The method could be directly used to ensure compliance with the maximum contaminant level (MCL) of mercury ion in drinking water set by regulations [35,36]. Linearities were studied based on standard mixtures at seven concentration levels, typically from 5 to at least 2500 LODs. The square correlation coefficients (r^2) for all the calibration graphs were higher than 0.994 (Fig. S6), suggesting the good linearity of the method. Repeatability of the method was expressed as the relative standard deviation (RSD) of migration time and peak area of each metal ion. The intra-day RSD values, based on five consecutive runs each day, were $<2.06\%$ for migration times and $<11.79\%$ for peak areas; the corresponding values were $<2.81\%$ and $<12.87\%$ for inter-day repeatability, which were estimated on three consecutive days. The effect of anions of the sample matrix was also evaluated. The electropherograms of metal ions prepared in different anions (chloride, nitrate and sulfate) did not show significant differences (Supplementary information, Fig. S7), suggesting the applicability of the method for varying sample matrices.

The recoveries of the metal ions from the real water samples, determined on three concentration levels, were in the range of 86.7–108.5% (Table 2). The concentrations of heavy metal ions in snow, tap and rain water samples determined by this method (Fig. 5) agreed well with the certified values (from ICP-MS). Based on the above assessment, the method is sensitive, of good reproducibility and accuracy, and can be applied to simultaneous determination of toxic metals in real water sample matrices.

4. Conclusions

Ester-terminated PAMAM G 2.5 dendrimers were synthesized and their potential application in CE analysis of heavy metal ions was investigated. By forming M–PAMAM chelates, PAMAM molecules could sweep and, therefore, stack the heavy metal ions, providing significant improvement in detectability. The second sweeping by PAR in the buffer, by forming more stable M–PAR chelates, further stacked the ions. During separation, PAMAM immobilized on the inner capillary surface served as stationary phase, providing selectivity toward and suppressing the adsorption of the solutes. The hyphenated dual sweeping-OTCEC strategy enabled rapid and sensitive determination of heavy metal ions in real water samples. The method is selective compared with the widely reported CE-conductivity detection in which large quantity of alkali metal ions in sample matrix may be interferences. Moreover, the method developed can directly, accurately detect mercury at sub μg/L level without laborious off-column preconcentration or derivation, and can be used by regulatory agencies to ensure compliance with the maximum contaminate level of this metal allowed in water samples.

Acknowledgments

The authors gratefully acknowledge the supports from the National Natural Science Foundation of China (20975014) and the Fundamental Research Funds for the Central Universities.

Appendix A. Supplementary material

Supplementary data associated with this article can be found in the online version at http://dx.doi.org/10.1016/j.talanta.2013.12.041.

References

[1] H.F. Lau, N.M. Quek, W.S. Law, J.H. Zhao, P.C. Hauser, S.F.Y. Li, Electrophoresis 32 (2011) 1190–1194.
[2] J. Petr, S. Gerstmann, H. Frank, J. Sep. Sci. 29 (2006) 2256–2260.
[3] X.B. Yin, J. Chromatogr. A 1154 (2007) 437–443.
[4] F. Tan, B.C. Yang, Y.F. Guan, Anal. Sci. 21 (2005) 955–958.
[5] W. Zhang, J.F. Chen, L.Y. Fan, C.X. Cao, J.C. Ren, S. Li, J. Shao, Analyst 135 (2010) 140–148.
[6] K. Isoo, S. Terabe, Anal. Sci. 21 (2005) 43–47.
[7] J.P. Quirino, S. Terabe, Anal. Chem. 70 (1998) 149–157.
[8] J.P. Quirino, J.B. Kim, S. Terabe, J. Chromatogr. A 965 (2002) 357–373.
[9] O.A. Matthews, A.N. Shipway, J.F. Stoddart, Prog. Polym. Sci. 23 (1998) 1–56.
[10] X. Shi, I. Banyai, K. Rodriguez, M.T. Islam, W. Lesniak, P. Balogh, L.P. Balogh, J.R. Baker, Electrophoresis 27 (2006) 1758–1767.
[11] P. Sedlakova, J. Svobodova, I. Miksik, H. Tomas, J. Chromatogr. B 841 (2006) 135–139.
[12] N. Tanaka, T. Fukutome, K. Hosoya, K. Kimata, T. Araki, J. Chromatogr. A 716 (1995) 57–67.
[13] A.L. Graya, J.T. Hsub, J. Chromatogr. A 824 (1998) 119–124.
[14] S.A. Kuzdzal, C.A. Monnig, G.R. Newkome, C.N. Moorefield, J. Am. Chem. Soc. 119 (1997) 2255–2261.
[15] M. Castagnola, L. Cassiano, A. Lupi, I. Messana, M. Patamia, R. Rabino, D.V. Rossetti, B. Giardina, J. Chromatogr. A 694 (1995) 463–469.
[16] C. Stathakis, E.A. Arriaga, N.J. Dovichi, J. Chromatogr. A 817 (1998) 233–238.
[17] Q.C. Liu, J. Tian, C.L. Zhang, H. Yang, Y. Liu, W.D. Qin, Z.P. Liu, Electrophoresis 32 (2011) 1302–1308.
[18] J. Tian, J.P. Qiao, J.J. Gao, W.D. Qin, J. Chromatogr. A 1280 (2013) 112–116.
[19] M.S. Diallo, S. Christie, P. Swaminathan, L. Balogh, X.Y. Shi, W. Um, C. Papelis, W.A. Goddard, J.H. Johnson, Langmuir 20 (2004) 2640–2651.
[20] M.R. Mankbadi, M.A. Barakat, M.H. Ramadan, H.L. Woodcock, J.N. Kuhn, J. Phys. Chem. B 115 (2011) 13534–13540.
[21] D. Shcharbin, J. Mazur, M. Szwedzka, M. Wasiak, B. Palecz, M. Przybyszewska, M. Zaborski, M. Bryszewska, Coll. Surf. B 58 (2007) 286–289.
[22] D.A. Tomalia, H. Baker, J. Dewald, M. Hall, G. Kallos, S. Martin, J. Roeck, J. Ryder, P. Smith, Polym. J. 17 (1985) 117–132.
[23] C. Zhang, Y. Zhang, W. Qin, Food Anal. Methods 7 (2014) 165–171.
[24] ⟨https://www.beckmancoulter.com/wsrportal/wsrportal.portal?_nfpb=true&_windowLabel=UCM_RENDERER&_urlType=render&wlpUCM_RENDERER_page=softwareInstructionPage&softwareId=8&softwareInstructionId=130⟩ (accessed 18.12.13).
[25] Z. Liu, H.F. Zou, M.L. Ye, J.Y. Ni, Y.K. Zhang, Electrophoresis 20 (1999) 2891–2897.
[26] F.B. Regan, M.P. Meaney, S.M. Lunte, J. Chromatogr. B 657 (1994) 409–417.
[27] N. Iki, H. Hoshino, T. Yotsuyanagi, Chem. Lett. (1993) 701–704.
[28] W.J. Geary, G. Nickless, F.H. Pollard, Anal. Chim. Acta 26 (1962) 71–79.
[29] R.C. Dunbar, J.D. Steill, N.C. Polfer, J. Oomens, J. Phys. Chem. A 113 (2009) 845–851.
[30] B. Harman, I. Sovago, Inorg. Chim. Acta—Bioinorg. Chem. 80 (1983) 75–83.
[31] V. Cucinotta, R. Caruso, A. Giuffrida, M. Messina, G. Maccarrone, A. Torrisi, J. Chromatogr. A 1179 (2008) 17–23.
[32] S. Tokalioglu, O. Dasdelen, Clean—Soil Air Water 39 (2011) 296–300.
[33] P. Kuban, P. Houserova, P. Kuban, P.C. Hauser, V. Kuban, J. Sep. Sci. 30 (2007) 1070–1076.
[34] A. Riaz, D.S. Chung, Electrophoresis 26 (2005) 668–673.
[35] Ministry of Health, Standardization Administration of the People's Republic of China, Standards for Drinking Water Quality, GB 5749-2006, 2007.
[36] US EPA, National Primary Drinking Water Regulations, United States Environmental Protection Agency, EPA 816-F-09-004,2009.